J|A|C|S
ARTICLES
Published on Web 03/04/2005

Binding Mode and Transcriptional Activation Potential of High Affinity Ligands for the CBP KIX Domain

Heather M. Volkman,[†] Stacey E. Rutledge,[†,§] and Alanna Schepartz*[,†,‡]

Contribution from the Department of Chemistry and Department of Molecular, Cellular and Developmental Biology, Yale University, New Haven, Connecticut 06520-8107

Received December 1, 2004; E-mail: Alanna.Schepartz@yale.edu

Abstract: We recently described a pair of ligands, PPKID4^{P} (**4^{P}**) and PPKID6^{U} (**6^{U}**), which present the α-helical functional epitope found on helix B of the CREB KID activation domain (KID^{P}) on a pancreatic fold protein scaffold. **4^{P}** and **6^{U}** bind the natural target of KID^{P}, the KIX domain of the coactivator CBP, with equilibrium dissociation constants between 515 nM and 1.5 μM and compete effectively with KID^{P} for binding to CBP KIX (KIX).[1] Here we present a detailed investigation of the binding mode, orientation, and transcriptional activation potential of **4^{P}** and **6^{U}**. Equilibrium binding experiments using a panel of well-characterized KIX variants support a model in which **4^{P}** binds KIX in a manner that closely resembles that of KID^{P} but **6^{U}** binds an overlapping, yet distinct region of the protein. Equilibrium binding experiments using a judiciously chosen panel of **4^{P}** variants containing alanine or sarcosine substitutions along the putative α- or PPII helix of **4^{P}** support a model in which **4^{P}** folds into a pancreatic fold structure upon binding to KIX. Transcriptional activation assays performed in HEK293 cells using GAL4 DNA-binding domain fusion proteins indicate that **4^{P}** functions as a potent activator of p300/CBP-dependent transcription. Notably, **6^{U}** is a less potent transcriptional activator in this context than **4^{P}** despite the similarity of their affinities for CBP KIX. This final result suggests that thermodynamic affinity is an important, although not exclusive, criterion controlling the level of KIX-dependent transcriptional activation.

Introduction

There is considerable current interest in the design or discovery of molecules capable of binding protein surfaces and inhibiting the formation of transient protein−protein interactions inside the cell.[2−4] Molecules with these properties can report on the functional relevance of discrete protein interactions and have potential as therapeutic leads for the large fraction of the genome currently considered "undruggable". Over the past few years our laboratory has developed a miniature protein-based strategy for the identification of high affinity ligands for protein-interaction surfaces and demonstrated that these molecules can function as potent and selective protein−protein interaction inhibitors.[1,5−7] This strategy makes use of the small but well-folded protein avian pancreatic polypeptide (aPP)[8] as a scaffold for the presentation and stabilization of an α-helical or PPII-helical binding epitope. This procedure, used with[1,5,7,9] or without[6,10,11] directed evolution, has successfully identified miniature protein ligands possessing nanomolar affinities for an array of protein and duplex DNA targets. These targets include the DNA sequences recognized by GCN4[9,10] and the Q50K variant of the *engrailed* homeodomain,[11] the related antiapoptotic proteins Bcl-2 and Bcl-X_L,[5,7] the oncoprotein hDM2,[12] and the EVH1 domain of the cytoskeletal protein Mena.[6] The most striking feature of well characterized protein surface ligands derived from aPP is their ability to discriminate the desired target from other macromolecules, even those that are extremely close in sequence, structure, or both.[5−7,9] Recently, our miniature protein design strategy was applied by Shimba and co-workers[13] to generate an aPP-based ligand for the Karposi sarcoma-associated herpesvirus protease that inhibited protein dimerization with an affinity in the micromolar concentration range and by Cobos et al.[14] to generate a 20 μM ligand for the Abl SH3 domain.

Recently we applied our miniature protein design strategy to identify a set of molecules that recognize a shallow surface cleft on the transcriptional coactivator CBP (the KIX domain) with

[†] Department of Chemistry.
[‡] Department of Molecular, Cellular and Developmental Biology.
[§] Present address: Centre for Protein Engineering, Medical Research Council Centre, Hills Road, Cambridge CB2 2QH, UK.

(1) Rutledge, S. E.; Volkman, H. M.; Schepartz, A. *J. Am. Chem. Soc.* **2003**, *125*, 14336.
(2) Cochran, A. G. *Curr. Opin. Chem. Biol.* **2001**, *5*, 654.
(3) Sidhu, S. S.; Bader, G. D.; Boone, C. *Curr. Opin. Chem. Biol.* **2003**, *7*, 97.
(4) Arkin, M. R.; Wells, J. A. *Nat. Rev. Drug Discov.* **2004**, *3*, 301.
(5) Chin, J. W.; Schepartz, A. *Angew. Chem., Int. Ed.* **2001**, *40*, 3806.
(6) Golemi-Kotra, D.; Mahaffy, R.; Footer, M. J.; Holtzman, J. H.; Pollard, T. D.; Theriot, J. A.; Schepartz, A. *J. Am. Chem. Soc.* **2004**, *126*, 4.
(7) Gemperli, A. C.; Rutledge, S. E.; Maranda, A.; Schepartz, A. *J. Am. Chem. Soc.* **2005**, *127*, 1596.
(8) Blundell, T.; Pitts, J.; Tickle, I.; Wood, S.; Wu, C.-W. *Proc. Natl. Acad. Sci. U.S.A.* **1981**, *78*, 4175.
(9) Chin, J. W.; Schepartz, A. *J. Am. Chem. Soc.* **2001**, *123*, 2929.
(10) Zondlo, N. J.; Schepartz, A. *J. Am. Chem. Soc.* **1999**, *121*, 6938.
(11) Montclare, J. K.; Schepartz, A. *J. Am. Chem. Soc.* **2003**, *125*, 3416.
(12) Kritzer, J. A.; Zutshi, R.; Cheah, M.; Ran, F. A.; Webman R.; Wongjirad, T. M.; Schepartz, A. Manuscript in preparation.
(13) Shimba, N.; Nomura, A. M.; Marnett, A. B.; Craik, C. S. *J. Virol.* **2004**, *78*, 6657.
(14) Cobos, E. S.; Pisabarro, M. T.; Vega, M. C.; Lacroix, E.; Serrano, L.; Ruiz-Sanz, J.; Martinez, J. C. *J. Mol. Biol.* **2004**, *342*, 355.

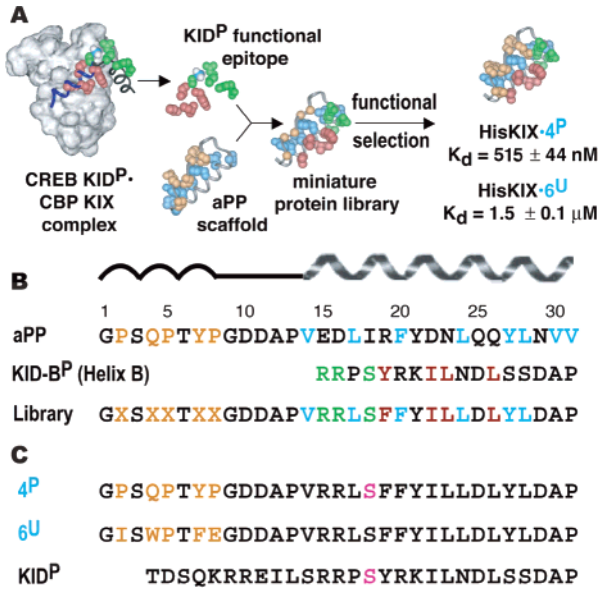

Figure 1. (A) Design and discovery of PPKID4^{P} (**4^{P}**) and PPKID6^{U} (**6^{U}**), two high affinity ligands for the KIX domain of CBP.[1] In the KID^{P}·KIX complex,[15] the backbone of KID-B^{P} is in blue, the residues along helix B that comprise the functional epitope are in red, and the PKA recognition site used to direct the PKA-dependent phosphorylation of serine is in green. (B) Alignment of the sequences of aPP, KID-B^{P} (residues 130−146), and the library used to identify **4^{P}** and **6^{U}**.[1] Residues along the α- and PPII-helices that contribute to formation of the aPP hydrophobic core are in blue and orange, respectively, residues important for binding KIX are in red, and residues that comprise the PKA recognition site are in green. Residues randomized in the library are indicated by X. (C) The sequences of **4^{P}**, **6^{U}**, and KID^{P}. Selected residues are in orange, and the phosphorylated serine residues are in pink.

high nanomolar to low micromolar affinity (Figure 1A).[1] These molecules were identified from a phage library of phosphorylated or unphosphorylated aPP variants containing the α-helical epitope from helix B of the CREB KID domain (the KID^{P} functional epitope) (Figure 1B). The highest affinity phosphorylated and unphosphorylated ligands for CBP KIX (abbreviated KIX henceforth) identified in this work are shown in Figure 1C. [Throughout this work, phosphorylated ligands are indicated by a superscript P and unphosphorylated ligands are indicated by a superscript U.] The phosphorylated ligand PPKID4^{P} (abbreviated **4^{P}** henceforth) binds KIX as well as the KID domain of CREB (abbreviated **KID^{P}**), with an equilibrium affinity of 515 ± 44 nM for KIX.[1] The unphosphorylated ligand PPKID6^{U} (abbreviated **6^{U}** henceforth) binds KIX with an equilibrium affinity of 1.5 ± 0.1 μM.[1] Both **4^{P}** and **6^{U}** compete with **KID^{P}** for binding to KIX in fluorescence polarization experiments. Moreover, the results of extensive competition experiments indicate that **4^{P}** and **6^{U}** exhibit high specificity for KIX over proteins that bind hydrophobic or α-helical molecules, such as carbonic anhydrase and calmodulin.[1]

In this work we explore in detail the binding mode and orientation of **4^{P}** and **6^{U}** on the surface of KIX and evaluate the ability of these ligands to function as transcriptional activation domains in cultured mammalian cells. Binding mode and orientation were explored with a set of twelve well-characterized KIX variants in which one residue within the **KID^{P}** binding groove was substituted by alanine.[16] The relative affinities of these twelve variants for **4^{P}**, **6^{U}**, and **KID^{P}** provided a large, consistent data set describing the free energy landscapes of the three KIX complexes. The data support a model in which the phosphorylated ligands **4^{P}** and **KID^{P}** bind KIX with virtually identical footprints, whereas the unphosphorylated ligand **6^{U}** binds an overlapping but distinct region of the protein. Next we made use of a set of eleven **4^{P}** variants in which one residue was substituted by alanine and/or sarcosine to probe the conformation of **4^{P}** when bound to KIX. The relative affinities of these variants support a model in which **4^{P}** folds into an aPP-like conformation upon binding to KIX. In an attempt to correlate binding mode and orientation to biological function, we next determined the potencies of **4^{P}** and **6^{U}** as artificial activation domains when fused to a heterologous DNA-binding domain. Transcription assays performed in HEK293 cells indicate that **4^{P}** activates transcription at a level comparable to **KID^{P}** through a p300/CBP-dependent mechanism. Surprisingly, **6^{U}** does not activate transcription, but phosphorylation converts this ligand into a moderate activation domain. These results suggest that equilibrium binding affinity and binding mode both contribute to transcriptional activation potency in the context of CBP and CREB.

Results

Do 4^{P} and 6^{U} Occupy the CREB KID Site on KIX? In our previous work, we reported that both **4^{P}** and **6^{U}** bind wild-type KIX with high affinity.[1] In the case of the phosphorylated ligand **4^{P}**, the affinity for KIX (515 ± 44 nM) was comparable to that of the full length phosphorylated CREB KID domain (**KID^{P}**, K_d = 562 ± 41 nM), whereas the affinity of the unphosphorylated ligand **6^{U}** for KIX was approximately 3-fold lower (K_d = 1.5 ± 0.1 μM) than that of KID-AB^{P}.[1] To further explore the binding location and orientation of **4^{P}** and **6^{U}**, we made use of a set of twelve well-studied KIX variants.[16] These twelve KIX variants each contain a single alanine substitution within or around the CREB-binding groove, and their affinities for **KID^{P}** span a 3.7 kcal mol^{-1} range (Table 1). We reasoned that if **4^{P}** and **6^{U}** interact with KIX in a manner that mimics that of **KID^{P}**, whose interactions with KIX have been characterized in detail by NMR,[15] then their affinities for these twelve variants should parallel one another. The twelve KIX variants were expressed in *E. coli* as fusions with glutathione-*S*-transferase to aid purification, and the GST tag was removed prior to analysis. The relative affinities of **KID^{P}**, **4^{P}**, and **6^{U}** for the panel of KIX variants, as well as for an analogous protein containing the wild-type KIX sequence (KIX), were measured by equilibrium fluorescence polarization (Figure 2 and Table 1). The affinities of **KID^{P}**, **4^{P}**, and **6^{U}** for KIX (Table 1) agree well with the affinities for HisKIX measured previously.[1]

Comparison of the Binding Modes of 4^{P} and KID^{P}. A. Recognition of Phosphoserine. Recognition of the phosphoserine residue in **KID^{P}** by Y658 and K662 in KIX contributes significantly to the stability of the KID·KIX complex, with energetic contributions between 1.5 and 4 kcal mol^{-1}.[16−18] Therefore we first evaluated the extent to which recognition of the **4^{P}** phosphoserine contributes to the binding energy of the

(15) Radhakrishnan, I.; Perez-Alvarado, G. C.; Parker, D.; Dyson, H. J.; Montminy, M. R.; Wright, P. E. *Cell* **1997**, *91*, 741.

(16) Parker, D.; Jhala, U. S.; Radhakrishnan, I.; Yaffe, M. B.; Reyes, C.; Shulman, A. I.; Cantley, L. C.; Wright, P. E.; Montminy, M. *Mol. Cell* **1998**, *2*, 353.
(17) Mestas, S. P.; Lumb, K. J. *Nat. Struct. Biol.* **1999**, *6*, 613.
(18) Zor, T.; Mayr, B. M.; Dyson, H. J.; Montminy, M. R.; Wright, P. E. *J. Biol. Chem.* **2002**, *277*, 42241.

Table 1. Equilibrium Dissociation Constants of the Complexes between **4^{P}**, **6^{U}**, and **KID^{P}** and Selected KIX Variants

	KID^{P}		4^{P}		6^{U}	
KIX	K_d (μM)	$\Delta\Delta G$ (kcal mol^{-1})	K_d (μM)	$\Delta\Delta G$ (kcal mol^{-1})	K_d (μM)	$\Delta\Delta G$ (kcal mol^{-1})
wild-type KIX	0.41 ± 0.04		0.61 ± 0.04		0.54 ± 0.06	
phosphoserine contact substitutions						
Y658A	142 ± 12	3.5	3.9 ± 0.3	1.1	1.7 ± 0.4	0.68
Y658F	26 ± 5	2.5	4.1 ± 0.2	1.1	2.8 ± 0.4	0.97
K662A	4.8 ± 0.4	1.5	3.9 ± 0.3	1.1	1.8 ± 0.3	0.71
hydrophobic contact substitutions (within binding cleft)						
L599A	1.1 ± 0.1	0.58	1.6 ± 0.1	0.58	3.3 ± 0.3	1.1
L603A	3.4 ± 0.3	1.2	3.4 ± 0.5	1.0	2.5 ± 0.3	0.91
K606A	2.3 ± 0.2	1.0	3.1 ± 0.2	0.97	1.2 ± 0.1	0.47
Y650A	9.4 ± 0.7	1.8	3.0 ± 0.3	0.95	1.3 ± 0.2	0.52
LL652-3AA	2.9 ± 0.2	1.2	2.9 ± 0.2	0.93	0.14 ± 0.02	−0.80
I657A	1.9 ± 0.1	0.90	2.7 ± 0.1	0.89	3.6 ± 0.4	1.1
hydrophobic contact substitutions (outside cleft)						
E655A	0.71 ± 0.05	0.32	0.54 ± 0.05	−0.07	1.7 ± 0.2	0.68
I660A	0.27 ± 0.03	−0.26	1.1 ± 0.1	0.35	6.1 ± 0.7	1.4
Q661A	0.93 ± 0.07	0.48	1.1 ± 0.1	0.35	0.41 ± 0.06	−0.16

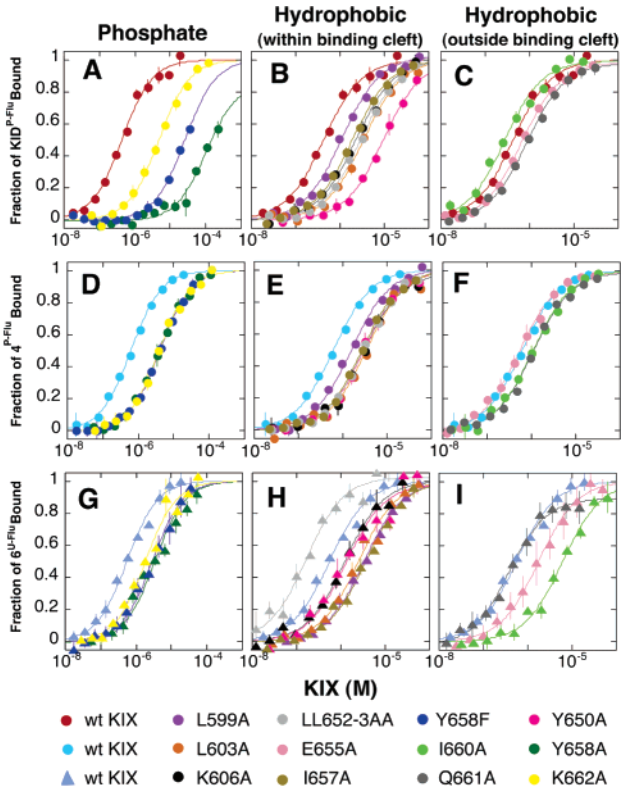

Figure 2. Binding isotherms illustrating the equilibrium affinities of **4^{P}**, **6^{U}**, and **KID^{P}** for KIX variants as determined by fluorescence polarization analysis at 25 °C. Each plot illustrates the fraction of 25 nM **KID^{P}** (A−C), **4^{P}** (D−F), or **6^{U}** (G−I) bound as a function of the molar concentration of KIX variant. Observed polarization values were converted to fraction of ligand^{Flu} bound using P_{min} and P_{max} values derived from the best fit of the polarization data to eq 1. Curves shown represent the best fit of the data to eq 2. Phosphorylated ligands are indicated with circles, whereas unphosphorylated ligands are indicated by triangles. Each point represents an average of three independent trials; error bars denote standard error.

4^{P}·KIX complex by examining two KIX variants containing phenylalanine and/or alanine in place of Y658 and K662 (Figure 3A). In the solution structure of **KID^{P}** bound to KIX, the KIX Y658 side chain donates a phenolic hydrogen bond to one terminal phosphoserine oxygen on **KID^{P}** and the K662 ammonium group forms a salt bridge to a second.[15,16] Y658F and K662A KIX both bind **KID^{P}** with significantly lower affinity than does wild-type KIX, consistent with previous results,[16] to form complexes with equilibrium dissociation constants of 26 ± 5 and 4.8 ± 0.4 μM, respectively. These K_d values correspond to binding free energies that are 2.5 and 1.5 kcal mol^{-1} less favorable, respectively, than that of the wild type **KID^{P}**·KIX complex. The free energy changes measured for these two variants, as well as for the Y658A variant (discussed below), are consistent with previous work and are fully supported by the **KID^{P}**·KIX structure.[15,16]

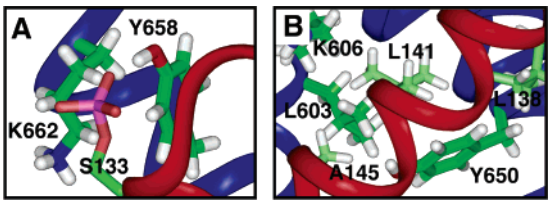

Figure 3. Close-up view of (A) phosphoserine and (B) hydrophobic contacts in the **KID^{P}**·KIX complex.[15] The backbones of **KID^{P}** and KIX are shown as red and blue ribbons, respectively; the side chains of Y658, K662, L603, K606, and Y650 (from KIX) and S133, L138, L141, and A145 (from **KID^{P}**) are shown explicitly.

Y658F and K662A KIX also bind **4^{P}** with significantly lower affinity than does the wild-type KIX protein. The equilibrium dissociation constant of the **4^{P}**·Y658F complex is 4.1 ± 0.2 μM, corresponding to a binding free energy that is 1.1 kcal mol^{-1} less favorable than that of the **4^{P}**·KIX complex. This value of $\Delta\Delta G$ is approximately one-half the value calculated in the case of the **KID^{P}**·Y658F complex. The equilibrium dissociation constant of the **4^{P}**·K662A complex is 3.9 ± 0.3 μM, corresponding to a binding free energy that is 1.1 kcal mol^{-1} less favorable than that of the wild type **4^{P}**·KIX complex. This value of $\Delta\Delta G$ is virtually identical to the value calculated in the case of the **KID^{P}**·K662A complex. Thus, both Y658 and K662 contribute significantly to the affinity of KIX for **4^{P}**, although the relative contributions of these two residues may differ between the **KID^{P}**·KIX and **4^{P}**·KIX complexes.

We also examined the affinities of **KID^{P}** and **4^{P}** for the Y658A variant of KIX, in which the Y658 side chain is replaced

by alanine. The NMR structure of the **KID^P**·KIX complex shows the Y658 aromatic ring packed against the side chain of L128, which is located on helix A of **KID^P**.[15] Y658A KIX binds **KID^P** with exceptionally low affinity ($K_d = 142 \pm 12$ μM), a loss in binding free energy of 3.5 kcal mol^{-1}. Presumably the large value of $\Delta\Delta G$ results from loss of contributions from both the Y658 hydroxyl group and aromatic ring. Since **4^P** lacks any residue corresponding to L128 on helix A, one would expect the stability of the **4^P**·Y658A complex to be comparable to that of the **4^P**·Y658F complex. Indeed, the equilibrium dissociation constant of the **4^P**·Y658A complex is 4.1 ± 0.2 μM, corresponding to a free energy loss of 1.1 kcal mol^{-1}, a value identical to that measured for the **4^P**·Y658F complex.

B. Hydrophobic Contacts. Next we considered those residues that line the shallow **KID^P** binding cleft on KIX. Six of the twelve variants (L599A, L603A, K606A, Y650A, LL652-3AA, and I657A) contain alanine in place of a residue within this cleft. For example, Y650 of KIX comprises one face of the binding cleft and interacts with three hydrophobic side chains of **KID^P**, L138, L141, and A145 (Figure 3B).[15] The Y650A variant binds **KID^P** with significantly reduced affinity ($K_d = 9.4 \pm 0.7$ μM), corresponding to a 1.8 kcal mol^{-1} loss in binding energy. Together, residues L603 and K606 form one side of the KIX binding cleft, interacting with **KID^P** residues L141 and A145. The L603A and K606A KIX variants bind **KID^P** with equilibrium dissociation constants of 3.4 ± 0.3 and 2.3 ± 0.2 μM, corresponding to binding free energy losses of 1.2 and 1.0 kcal mol^{-1} compared to **KID^P**·KIX. Other KIX residues that comprise part of the hydrophobic cleft are L653 and I657; both interact with **KID^P** residue L141 in addition to other residues. As expected, LL652-3AA and I657A KIX bind **KID^P** with lower affinity ($K_d = 2.9 \pm 0.2$ and 1.9 ± 0.1 μM), corresponding to binding free energy losses of 1.2 and 0.9 kcal mol^{-1}, respectively. Located at the bottom of the binding cleft, residue L599 interacts with only one residue, P146, of **KID^P**. The L599A variant binds **KID^P** with lower affinity, but the free energy loss in this case is smaller than that observed with other variants with substitutions in the hydrophobic cleft; the **KID^P**·L599A complex is characterized by an equilibrium dissociation constant of 1.1 ± 0.1 μM, a binding free energy loss of 0.58 kcal mol^{-1}. In summary, all six KIX variants with side chain substitutions at positions that participate in hydrophobic contacts with **KID^P**, as judged by NMR,[15] bind **KID^P** with diminished affinity.

The six KIX variants with substitutions in the hydrophobic cleft also show diminished affinity for **4^P**, with equilibrium dissociation constants between 1.6 ± 0.1 and 3.4 ± 0.5 μM (Figure 2E, Table 1). These K_d values correspond to the free energy changes ($\Delta\Delta G$) that range between 0.58 and 1.0 kcal mol^{-1}, values that are, with one exception, in close agreement with those measured for the analogous complexes with **KID^P**. The one exception to this trend is Y650A KIX, whose complex with **KID^P** is 1.8 kcal mol^{-1} less stable than the complex with wild-type KIX. By contrast, the **4^P**·Y650A complex is only 0.95 kcal mol^{-1} less stable than the complex with wild-type KIX.

C. Residues Surrounding the Binding Pocket. In addition to the KIX variants described above, which contain mutations within the **KID^P** binding pocket, we also examined three variants, E655A, I660A, and Q661A, containing alanine in place of a residue that surrounds the **KID^P** binding pocket. We envisioned that analysis of these variants could report on subtle differences in the binding modes of **4^P** and **KID^P**. The equilibrium dissociation constants of the **KID^P** complexes of these three variants fall between 0.27 ± 0.03 and 0.93 ± 0.07 μM, values very close to that of the wild-type complex ($\Delta\Delta G = -0.26$ and $+0.48$ kcal mol^{-1}, respectively). These three KIX variants bind **4^P** with equilibrium dissociation constants between 0.54 ± 0.05 and 1.1 ± 0.1 μM, corresponding to free energy changes between -0.07 and 0.35 kcal mol^{-1}.

Comparison of the Binding Modes of 6^U and KID^P. A. Recognition of Phosphoserine. **6^U** lacks the phosphoserine that dominates the energetics of the **4^P**·KIX and **KID^P**·KIX interactions. Therefore, if **6^U** binds KIX in a manner mirroring that of **4^P** and **KID^P**, then we would expect it would be less sensitive to substitution of KIX residues that contact the **KID^P** phosphoserine, notably Y658 and K662. Surprisingly, **6^U** binds both Y658F and K662A KIX with significantly lower affinity than it binds wild-type KIX. The equilibrium dissociation constants of the **6^U**·Y658F and **6^U**·K662A complexes are 2.8 ± 0.4 and 1.8 ± 0.3 μM, corresponding to free energy losses of 0.97 and 0.71 kcal mol^{-1}, respectively, relative to the complexes with KIX. Interestingly, **6^U** binds the Y658A variant with higher affinity ($K_d = 1.7 \pm 0.4$ μM) than it binds the Y658F variant ($K_d = 2.8 \pm 0.4$ μM), whereas, as described above, **4^P** binds equally to Y658A and Y658F.

B. Hydrophobic Contacts. To further explore differences in the binding modes of **4^P** and **6^U**, we measured the affinity of **6^U** for KIX variants with substitutions of side chains that line the **KID^P** binding pocket (variants L599A, L603A, K606A, Y650A, and I657A) (Figure 2H and Table 1). Five of the six variants form complexes with **6^U** that are between 0.47 and 1.1 kcal mol^{-1} less stable than the wild-type **6^U**·KIX complex, whereas the complex with LL652-3AA is 0.8 kcal mol^{-1} more stable than the wild-type **6^U**·KIX complex. The largest differences in affinity for **6^U** are seen with L599A, L603A, and I657A KIX, with K_d values of 3.3 ± 0.3, 2.5 ± 0.3, and 3.6 ± 0.4 μM, respectively ($\Delta\Delta G = 1.1$, 0.91, and 1.1 kcal mol^{-1}, respectively). K606A and Y650A KIX bind **6^U** with affinities much closer to that of the wild-type complex ($K_d = 1.2 \pm 0.1$ and 1.3 ± 0.2 μM; $\Delta\Delta G = 0.47$ and 0.52 kcal mol^{-1}, respectively). Analysis of the differences in affinity among this set of **6^U**·KIX complexes reveals a pattern very different from that observed for the analogous **KID^P** or **4^P** complexes. For example, the Y650A and L599A variants form the most and least stable complexes, respectively, with **KID^P** and **4^P**, but the least and most stable complexes with **6^U**.

C. Residues Surrounding the Binding Pocket. Although KIX variants E655A, I660A, and Q661A display affinities for **KID^P** and **4^P** that are comparable to that of wild-type KIX, two of the variants show significantly diminished affinity for **6^U**. In particular, I660A and E655A KIX bind **6^U** poorly, with equilibrium dissociation constants of 6.1 ± 0.7 and 1.7 ± 0.2 μM and free energy losses of 1.4 and 0.68 kcal mol^{-1}, respectively. Q661A binds **6^U** with an affinity comparable to that of wild-type KIX. These differences in the relative and absolute contributions to stability among the KIX variants emphasize the differences in the binding modes of **4^P** and **6^U** irrespective of the ability of **6^U** to compete with **KID^P** for binding to wild-type KIX.

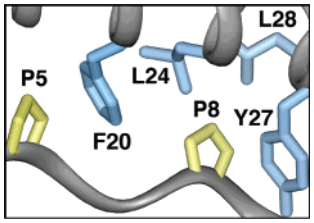

Figure 4. Close-up view of side chain packing in the aPP hydrophobic core, illustrating the relative orientation of F20, L24, Y27, and L28 on the α-helix (blue) and P3 and P5 on the PPII helix (yellow).[8]

Is 4^P Folded When Bound to KIX? The results described above support a model in which the α-helix in **4^P** is positioned within the KIX cleft in a manner that closely mimics that of **KID^P**. However, this model sheds no light on the conformation or location of the N-terminal proline-rich region of **4^P**, in particular, whether **4^P** is folded into an aPP-like hairpin conformation when bound. We previously reported that **4^P** displays only nascent α-helicity in water in the absence of KIX, as determined by circular dichroism, but that the extent of helicity increased in α-helix promoting solvents such as trifluoroethanol.[1] We hypothesized that if **4^P** folds into an aPP-like conformation upon binding to KIX, then the stability of the complex should depend on the presence of residues that comprise the intact hydrophobic core. To test this hypothesis, we prepared a set of eleven **4^P** variants in which alanine and/or sarcosine is substituted for a **4^P** residue that comprises the hydrophobic core in the putative folded state.[8] These variants include five with alanine substitutions along the face of the **4^P** α-helix that is located opposite the face used to contact KIX (L17A, F20A, L24A, Y27A, and L28A) and six with alanine or sarcosine substitutions along the PPII helix (P2A, P2Z, P5A, P5Z, P8A, and P8Z). A close-up view of packing in the hydrophobic core of aPP is shown in Figure 4.

4^P Variants Display a Range of Affinities for Wild-Type KIX. We used fluorescence polarization analysis to determine the KIX-binding affinities of eight **4^P** variants in which one residue within the putative hydrophobic core had been substituted with alanine. Five of these residues lie on the internal face of the aPP α−helix, whereas three lie on the internal face of the PPII helix. We also studied three variants in which a proline residue on the internal face of the PPII helix was substituted by sarcosine (Figure 5 and Table 2). The equilibrium dissociation constants of the **4^P** variant·KIX complexes range from 0.68 ± 0.05 to 3.09 ± 0.18 μM, corresponding to binding energies between 0.1 and 1.0 kcal mol^{-1} less favorable than the wild-type **4^P**·KIX complex. The stabilities of the complexes fall into three categories. The least stable complexes, containing variants F20A and Y27A, are 0.85 and 0.96 kcal mol^{-1} less stable than the wild-type **4^P**·KIX complex. Moderately stable complexes containing variants P5A, P8A, and L24A are 0.3 to 0.38 kcal mol^{-1} less stable than the wild-type **4^P**·KIX complex. Six of the variants, P2A, P2Z, P5Z, P8Z, L17A and L28A, formed complexes with KIX that are similar in energy (0.07 to 0.21 kcal mol^{-1}) to the wild-type **4^P**·KIX complex. When examined in the context of the folded structure of aPP itself, we find that those side chains that contribute significantly or moderately to **4^P**·KIX complex stability, F20, L24, Y27, P5, and P8, all lie at the center of the aPP hydrophobic core (Figure 4). In this structure[8] the aromatic side chain of F20 inserts between the side chains of P5 and P8, the branched side chain

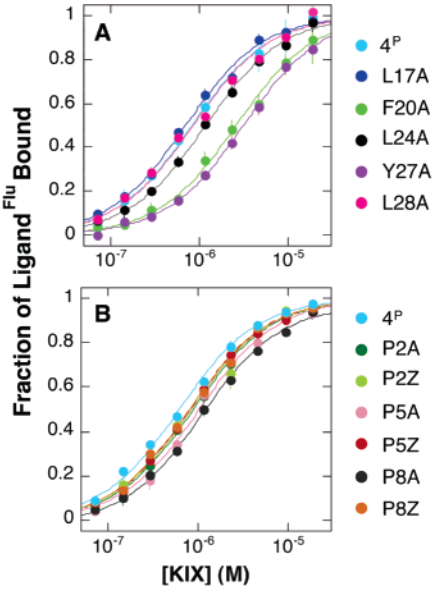

Figure 5. Binding isotherms illustrating the equilibrium affinities of **4^P** variants for KIX as determined by fluorescence polarization analysis at 25 °C. Each plot illustrates the fraction of 25 nM of the **4^P** variant bound as a function of the molar concentration of KIX. Each point represents an average of three independent trials. Observed polarization values were converted to fraction of ligand^{Flu} bound using P_{min} and P_{max} values derived from the best fit of the polarization data to eq 1. Curves shown are the best fit of fraction of ligand^{Flu} bound values to the equilibrium binding eq 2. (A) Binding isotherms for **4^P** variants L17A, F20A, L24A, Y27A, and L28A. (B) Binding isotherms for **4^P** variants P2A, P2Z, P5A, P5Z, P8A, and P8Z. Z indicates the substitution of sarcosine.

Table 2. Equilibrium Dissociation Constants of Complexes between **KIX** and **4^P** Variants As Determined by Fluorescence Polarization

4^P	K_d (μM)	$\Delta\Delta G$ (kcal mol^{-1})
wild-type	0.61 ± 0.04	
polyproline helix variants		
P2A	0.87 ± 0.04	0.21
P2Z	0.83 ± 0.08	0.18
P5A	1.02 ± 0.09	0.30
P5Z	0.80 ± 0.03	0.16
P8A	1.07 ± 0.08	0.33
P8Z	0.78 ± 0.05	0.15
α-helix variants		
L17A	0.68 ± 0.05	0.07
F20A	2.55 ± 0.25	0.85
L24A	1.16 ± 0.07	0.38
Y27A	3.09 ± 0.18	0.96
L28A	0.83 ± 0.11	0.18

of L24 packs against P8 and F20, and the side chain of Y27 packs against P8. By contrast, those side chains that contribute minimally to stability, P2, L17, and L28, lie at the edge of the aPP hydrophobic core and participate in fewer van der Waals interactions.

Can PPKID Peptides Function as Transcriptional Activation Domains in Cultured Cells? Eukaryotic transcriptional activators, such as CREB, stimulate gene expression primarily by recruitment of the general transcription machinery to the promoters of genes they regulate.[19] These transcription factors possess modular structures, containing both a specific DNA

(19) Ptashne, M.; Gann, A. *Genes & Signals*. Cold Spring Harbor Laboratory: New York, 2002.

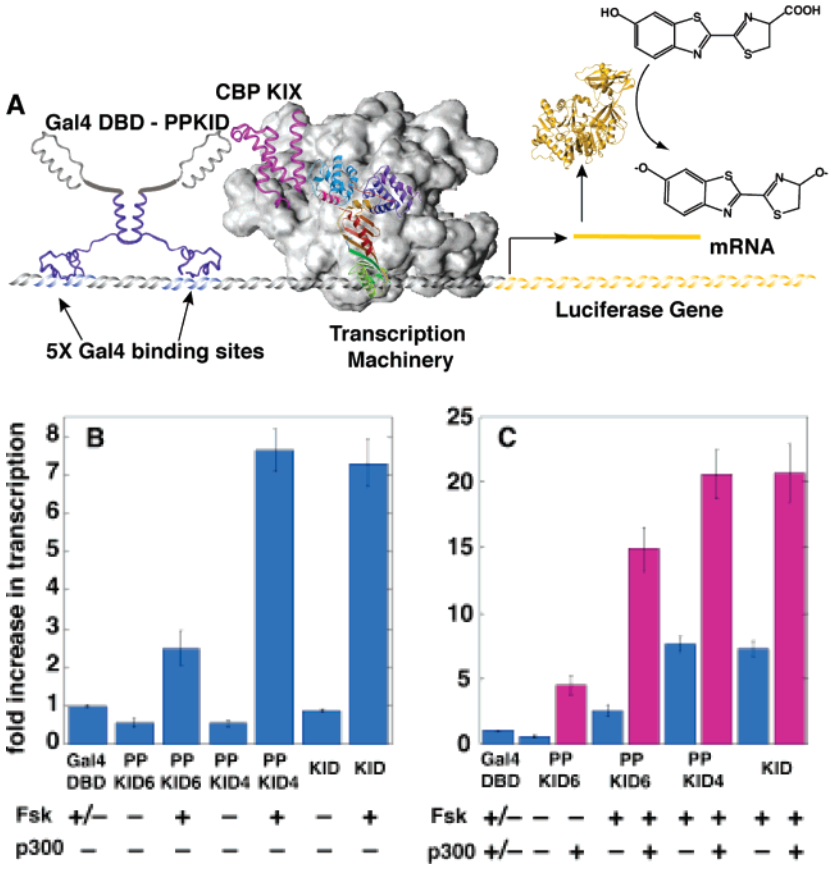

Figure 6. (A) Schematic of transcription reporter assay. (B and C) Transcriptional activation mediated by Gal4 DBD fusions of PPKID4, PPKID6, and KID in HEK293 cells in the absence (blue bars) or presence (pink bars) of exogenous p300. Bars and standard error represent results from at least three independent trials. Where indicated, 5 μM forskolin (Fsk) was added to the culture media 6 h prior to harvesting cells. When indicated, cells were also transfected with 25 ng CMV/p300-HA (p300), an expression vector encoding full-length p300 under control of the CMV promoter.[22] Expression of each Gal4 DBD fusion protein was verified using Western blots (see Supporting Information).

binding domain that targets the gene of interest and an activation domain that binds and recruits the transcriptional machinery. The functions of the DNA binding and transcriptional activation domains are separable and can be swapped among proteins within and outside a given family,[20,21] or replaced altogether with nonnatural counterparts,[22−24] to obtain molecules with novel and informative properties.[21] The development of fully artificial transcriptional activators is an important goal in chemical biology.[21] However, although there has been considerable success in the development of non-natural molecules that bind DNA with affinities and specificities that rival those of natural transcription factors,[9,11,23,25] the development of molecules that activate transcription has lagged considerably behind.[26] By virtue of their ability to bind CBP, a transcriptional coactivator protein that acts as a conduit between gene-specific activators and the basal transcription machinery, we hypothesized that $\mathbf{4}^{\mathbf{P}}$ and $\mathbf{6}^{\mathbf{U}}$ might function as artificial activation domains when fused to a heterologous DNA-binding domain.

To test this hypothesis and investigate the activation potential of these ligands, we prepared a series of mammalian expression plasmids, Gal4-KID, Gal4-PPKID4, and Gal4-PPKID6, in which the gene encoding the KIX ligands KID, PPKID4, or PPKID6, respectively, was fused to the C-terminus of the gene encoding the Gal4 DNA-binding domain (DBD) (residues 1−147). Gal4-KID, Gal4-PPKID4, and Gal4-PPKID6 are all derivatives of the previously reported expression vector pAL_1,[22] which directs the expression of the Gal4 DBD and was used as a control. Gal4-KID, Gal4-PPKID4, and Gal4-PPKID6 were introduced individually into HEK293 cells by transfection along with a previously described[27] reporter plasmid, G5B-luciferase, containing five Gal4 binding sites upstream of the firefly luciferase gene (Figure 6A). The cells were also transfected with a commercially available plasmid (pRL-null) encoding *Renilla* luciferase to normalize the data for differences in transfection efficiency. The *Renilla* and firefly luciferase enzymes utilize different substrates, facilitating the sequential analysis of both enzyme activities in a single sample. Transfected HEK293 cells were incubated at 37 °C for 36 h and lysed, and the ratio [R] of firefly and *Renilla* luciferase activities was measured using the Dual-Luciferase Reporter Assay System (Promega). The potency of each activation domain (fold activation) was determined by dividing the [R] values measured in cells transfected with Gal4-KID, Gal4-PPKID4, or Gal4-PPKID6 by the [R] value measured in cells transfected with pAL_1. Based on a previous study that observed a correlation between KIX-binding affinity and the activation potency of short peptides,[22] we expected $\mathbf{4}^{\mathbf{P}}$ and $\mathbf{6}^{\mathbf{U}}$

(20) Brent, R.; Ptashne, M. *Cell* **1985**, *43*, 729.
(21) Ansari, A. Z.; Mapp, A. K. *Curr. Opin. Chem. Biol.* **2002**, *6*, 765.
(22) Frangioni, J. V.; LaRiccia, L. M.; Cantley, L. C.; Montminy, M. R. *Nat. Biotechnol.* **2000**, *18*, 1080.
(23) Dervan, P. B.; Edelson, B. S. *Curr. Opin. Struct. Biol.* **2003**, *13*, 284.
(24) Minter, A. R.; Brennan, B. B.; Mapp, A. K. *J. Am. Chem. Soc.* **2004**, *126*, 10504.
(25) Beerli, R. R.; Barbas, C. F., III. *Nat. Biotechnol.* **2002**, *20*, 135.
(26) Mapp, A. K. *Org. Biomol. Chem.* **2003**, *1*, 2217.

would activate transcription at levels comparable to **KID^{P}** due to their similar affinities for KIX.

Activation Potential of 4$^{U/P}$, 6$^{U/P}$, and KID$^{U/P}$. First we investigated transcriptional activation potential of Gal4-PPKID4, Gal4-PPKID6, and Gal4-KID in the absence of forskolin treatment, conditions under which the phosphorylation of cellular proteins by PKA is not stimulated (Figure 6B). We previously reported that **4^{U}** and **KID^{U}** (which are not phosphorylated) possess low affinity ($K_d = 12.1 \pm 2.4$ μM and >116 μM) for KIX in vitro.[1] The level of firefly luciferase activity in cells transfected with 5 ng of Gal4-KID or Gal4-PPKID4 was, in the absence of forskolin, no higher than that in cells transfected with pAL$_1$ under identical conditions. Surprisingly, despite the fact that **6^{U}** possesses significant affinity ($K_d = 540 \pm 60$ nM) for KIX in vitro (Table 1), the level of firefly luciferase activity in cells transfected with 5 ng of Gal4-PPKID6 was also no higher than that in cells transfected with pAL$_1$ under identical conditions. The overall levels of firefly luciferase activity in cells transfected with Gal4-KID, Gal4-PPKID4, and Gal4-PPKID6 were typically between 50% and 90% of the levels obtained in cells transfected with pAL$_1$.

Next, we investigated the activation potential of Gal4-PPKID4, Gal4-PPKID6, and Gal4-KID after treatment with forskolin, conditions under which protein phosphorylation is stimulated.[28] Each of these ligands contains a serine residue in the context of an excellent PKA substrate,[29] and when phosphorylated synthetically, each possesses significantly greater affinity for KIX in vitro.[1] Therefore we expected that addition of forskolin to the cell culture media would result in the phosphorylation of PPKID4, PPKID6, and KID, leading to a commensurate increase in their potency as CBP-dependent transcriptional activators. Cells previously transfected with Gal4-KID, Gal4-PPKID4, or Gal4-PPKID6 were incubated with forskolin (0−100 μM) for various times to optimize the level of transcription activation; we found that a 6 h incubation with 5 μM forskolin led to the largest fold increase in transcriptional activation by Gal4-KID (7.5-fold), Gal4-PPKID4 (7.5-fold), and Gal4-PPKID6 (2.5-fold). Increasing the amount of Gal4-KID, Gal4-PPKID6, and Gal4-PPKID4 plasmids transfected (10−20 ng) did not further increase the level of transcription.

Does Transcriptional Activation by the PPKID Peptides Occur via the CBP/p300 Pathway? Previous work has demonstrated that transcriptional activation mediated by CREB occurs via recruitment of CBP to promoters where CREB is bound.[30] However, in the cell, transcription can be activated by a variety of different pathways.[31] To investigate whether Gal4-PPKID4 and Gal4-PPKID6 activate transcription in a CBP-dependent manner, we performed experiments in which HEK293 cells were transfected with the CMV/p300-HA plasmid[22] encoding the CBP paralog p300 as well as Gal4-KID, Gal4-PPKID4, or Gal4-PPKID6 and compared the level of transcription to that observed in absence of exogenous p300. Previous work has demonstrated that in the presence of exogenous CREB, components of the transcriptional machinery such as CBP are limiting,[32] hence an increase in the CBP/p300 concentration should lead to an increase in transcriptional activation that occurs via the CBP/p300 pathway.

As expected, coexpression of exogenous p300 along with Gal4-KID and treatment with forskolin led to a 20-fold increase in the level of transcription compared to the level observed in cells transfected with pAL$_1$, a 2.7-fold increase relative to the level observed in the absence of exogenous CBP/p300 (Figure 6C). The 2.7-fold increase observed in this work compares well with the 6-fold increase reported earlier for full-length CREB.[32] In the absence of forskolin, coexpression of exogenous p300 with Gal4-KID led to a 7.5-fold increase in the level of transcription (data not shown). Similarly, coexpression of exogenous p300 along with Gal4-PPKID4 and treatment with forskolin led to a 20-fold increase in the level of transcription compared to the level observed in cells transfected with pAL$_1$, a 2.7-fold increase relative to the level observed in the absence of exogenous p300. In the absence of forskolin, coexpression of exogenous p300 and Gal4-PPKID4 did not activate transcription (data not shown). Likewise, coexpression of exogenous p300 along with Gal4-PPKID6 and treatment with forskolin led to a 15-fold increase in the level of transcription compared to the level observed in cells transfected with pAL$_1$, a 6-fold increase relative to the level observed in the absence of exogenous p300. Somewhat surprisingly, addition of p300 also increased transcription activation by Gal4-PPKID6 in the absence of forskolin treatment to levels 4.5-fold over basal transcription levels, whereas Gal4-PPKID6 failed to activate transcription in the presence of only endogeous CBP/p300. Thus, although **6^{U}** is perhaps best described as a weak activation domain, it nevertheless activates transcription via the CBP/p300 pathway. These results are consistent with a model in which **4^{P}**, **6^{P}**, and **6^{U}**, like KID, activate transcription by recruitment of CBP/p300 via the KIX domain to the promoters where they are bound.

Transcription Inhibition by 4^{P}. The results presented above support a model in which Gal4-PPKID4 and Gal4-PPKID6 activate CBP-dependent transcription in a phosphorylation-dependent manner. This model suggests that **4^{P}** and **6^{P}**, when separated from the Gal4-DBD, should competitively inhibit transcription activated by proteins that interact with KIX. Therefore, to provide additional evidence of transcriptional activation via a CBP-dependent pathway, we analyzed the levels of transcription in forskolin-stimulated HEK293 cells transfected with 5 ng of Gal4-KID, Gal4-PPKID4, or Gal4-PPKID6 in the presence of increasing amounts (0−50 ng) of the pPPKID4 plasmid, encoding PPKID4 without the Gal4 DBD.

As expected, transcriptional activation was reduced from 7-fold to 3.5-fold when HEK293 cells were transfected with a 2:1 ratio of plasmids encoding PPKID4 and Gal4-PPKID4 and incubated in the presence of forskolin. Cotransfection of HEK293 cells with a 5:1 ratio of the two plasmids reduced the level of transcriptional activation by 100%, to the level observed when cells were transfected with the control plasmid pAL$_1$. Similarly, cotransfection of HEK293 cells with a 5:1 ratio of plasmids encoding PPKID4 and Gal4-KID reduced the level of transcriptional activation from 8-fold to 2-fold; transcription

(27) Kasper, L. H.; Brindle, P. K.; Schnabel, C. A.; Pritchard, C. E.; Cleary, M. L.; van Deursen, J. M. *Mol. Cell Biol.* **1999**, *19*, 764.
(28) Gonzalez, G. A.; Montminy, M. R. *Cell* **1989**, *59*, 675.
(29) Pearson, R. B.; Kemp, B. E. *Methods Enzymol.* **1991**, *200*, 62.
(30) Cardinaux, J. R.; Notis, J. C.; Zhang, Q.; Vo, N.; Craig, J. C.; Fass, D. M.; Brennan, R. G.; Goodman, R. H. *Mol. Cell Biol.* **2000**, *20*, 1546.
(31) Hochheimer, A.; Tjian, R. *Genes Dev.* **2003**, *17*, 1309.
(32) Kwok, R. P.; Lundblad, J. R.; Chrivia, J. C.; Richards, J. P.; Bachinger, H. P.; Brennan, R. G.; Roberts, S. G.; Green, M. R.; Goodman, R. H. *Nature* **1994**, *370*, 223.

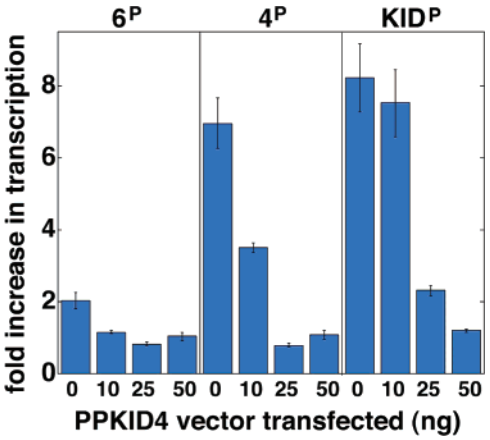

Figure 7. Inhibition of transcription by **4**^{P} in HEK293 cells. HEK293 cells were cotransfected with 5 ng of Gal4-KID, Gal4-PPKID4, or Gal4-PPKID6 expression plasmids and indicated amount of pPPKID4 (0−50 ng). Forskolin (5 μM) was added to culture media 6 h prior to harvesting cells. Bars and standard error represent the results from at least three independent trials. Fold increase in transcription was determined by dividing the [R] values measured in cells transfected with Gal4-KID, Gal4-PPKID4 or Gal4-PPKID6 by the [R] value measured in cells transfected with pAL_1 with each indicated amount of pPPKID4 to correct for any effect pPPKID4 has on basal transcription. On average, the addition of 50 ng of pPPKID4, in the presence of forskolin, decreased basal transcription 2-fold.

was completely inhibited when a 10:1 ratio was used. Due to its low level of activation, Gal4-PPKID6^{P} activation was reduced 100% when a 2:1 ratio of plasmids encoding PPKID4 and Gal4-PPKID6 were cotransfected in HEK293 cells and incubated in the presence of forskolin. These results also support a model in which **4**^{P} and **6**^{P} activate transcription in a CBP-dependent manner.

Discussion

Protein grafting is an adaptable strategy that has been used to identify miniature protein ligands for the DNA major groove,[9−11,33] deep protein clefts,[5] and certain PPII recognition domains.[6] With the identification of PPKID ligands for KIX, this approach was extended to the recognition of shallow protein surfaces.[1] Here we investigate in detail the binding mode of PPKID4^{P} (**4**^{P}) and PPKID6^{U} (**6**^{U}), the extent to which **4**^{P} assembles into an aPP-like conformation when bound, and the ability of PPKID4 and PPKID6 to recruit CBP and activate transcription in cultured mammalian cells.

Binding Mode and Orientation of CBP Ligands: PPKID4^{P}. Earlier work has shown that both **4**^{P} and **6**^{U} compete with the structurally well-characterized ligand KID^{P} for binding to KIX.[1] Although the observed competition supports an overlapping binding mode for these two ligands, it is also consistent with a nonoverlapping binding mode in which competition occurs through allostery. The results reported herein, using a broad panel of KIX variants, support a model in which the α-helix in **4**^{P} interacts with KIX in a manner very similar to the α-helix of **KID**^{P}. This conclusion is best illustrated by Figure 8, in which the free energy differences listed in Table 1, the differences in stability between the **KID**^{P} and **4**^{P} complexes of the KIX variants, are color-coded and mapped on the structure of KIX. In both cases, K662 and Y658, the KIX residues that contact phosphoserine, contribute most significantly to complex stability.

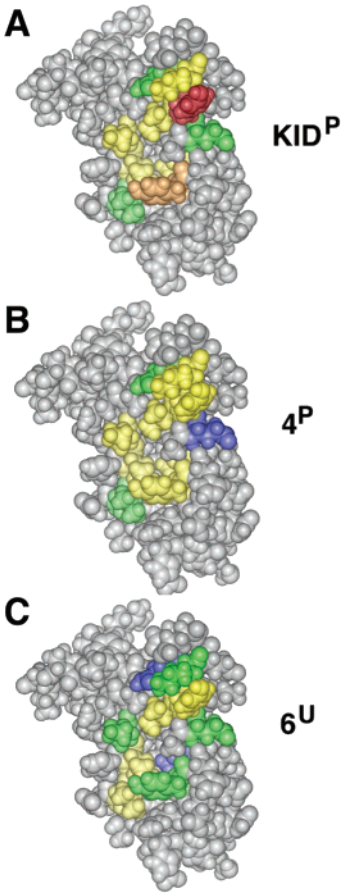

Figure 8. Relative stabilities of the KIX complexes of (A) **KID**^{P}, (B) **4**^{P}, and (C) **6**^{U} mapped on the structure of KIX. Residues are color-coded according to $\Delta\Delta G$ values listed in Table 1 in order to compare the extent to which complex stability is affected in the context of **KID**^{P}, **4**^{P}, and **6**^{U}. The substituted residues in complexes characterized by $\Delta\Delta G$ values between 2.5 and 3.5 kcal mol^{-1} are colored red, those in complexes characterized by $\Delta\Delta G$ values between 1.7 and 2.4 kcal mol^{-1} are colored orange, those in complexes characterized by $\Delta\Delta G$ values between 0.9 and 1.6 kcal mol^{-1} are colored yellow, those in complexes characterized by $\Delta\Delta G$ values between 0.3 and 0.8 kcal mol^{-1} are colored green, and those in complexes characterized by $\Delta\Delta G$ values < 0.3 kcal mol^{-1} are colored blue.

Residue K662 (shown in yellow) contributes virtually equally to the stabilities of the **KID**^{P} and **4**^{P} complexes with KIX ($\Delta\Delta G = 1.5$ and 1.1 kcal mol^{-1}, respectively), whereas Y658 (shown red in Figure 8A and in yellow in Figure 8B) contributes more to the stability of the complex with **KID**^{P} ($\Delta\Delta G = 2.5$ and 1.1 kcal mol^{-1}, respectively). Those KIX residues that line the hydrophobic cleft, contacting CREB L141 (L603, K606, Y650, L653, and I657, shown in yellow), with the exception of residue Y650, contribute more modestly but virtually equally to the stabilities of the **KID**^{P} and **4**^{P} complexes (Table 1). Finally, those KIX residues that contribute little (L599, Q661, and E655; shown in green) or not at all (I660; shown in blue) to the binding of **KID**^{P} also contribute little or not at all to the binding of **4**^{P} (L599, Q661 and I660 in green and E655 in blue). The observation that the free energies of the **4**^{P}·KIX complexes mirror those of the **KID**^{P}·KIX complexes provides strong evidence that the KIX residues in question contribute in a similar way to complex formation with the two ligands, supporting an analogous binding mode for the two ligands.

The parallels between the free energy landscapes of the **4**^{P} and **KID**^{P} complexes notwithstanding, two residues of KIX, Y658, which contacts the phosphoserine, and Y650, which

(33) Chin, J. W.; Grotzfeld, R. M.; Fabian, M. A.; Schepartz, A. *Bioorg. Med. Chem. Lett.* **2001**, *11*, 1501.

participates in hydrophobic interactions, contribute more heavily to **KID^{P}** complex formation than to **4^{P}** complex formation. In the context of **KID^{P}**, the amino acid changes embodied in the Y658F and Y650A KIX variants lead to complexes that are 2.5 and 1.8 kcal mol^{-1} less stable, respectively, than the wild-type complex, whereas in the context of **4^{P}** the corresponding free energy changes are 1.1 and 0.95 kcal mol^{-1}, respectively. Despite the diminished contributions of these two residues, KIX binds with equal affinity to **KID^{P}** and **4^{P}**. Taken together, these results suggest that an additional energetic factor contributes to the stability of the **4^{P}**·KIX complex but not the **KID^{P}**·KIX complex. As discussed below, one source for this additional factor is the free energy of folding **4^{P}** upon binding to KIX.

Binding Mode and Orientation of CBP Ligands: 6^{U}. The results reported herein support a model in which **6^{U}** interacts with KIX in a manner that overlaps, but is clearly distinguished from, that of either **4^{P}** or **KID^{P}**. Although the amino acid changes embodied in several KIX variants (L603A and I657A) lead to equivalent changes in **6^{U}** and **KID^{P}** complex stability, these variants are among the minority; the majority of variants form complexes with **6^{U}** whose stabilities are affected very differently than the complexes with **4^{P}** or **KID^{P}**. For example, variants with substitutions in the hydrophobic cleft surrounding CREB L141 (K606A, Y650A and L653A) form complexes with **6^{U}** whose stabilities are roughly equivalent to the corresponding complexes with wild-type KIX ($\Delta\Delta G = -0.8$ to $+0.5$ kcal·mol^{-1}), whereas the analogous complexes with **KID^{P}** or **4^{P}** are considerably less stable ($\Delta\Delta G = 1.0$ to 1.8 kcal mol^{-1} for **KID^{P}** complexes and $\Delta\Delta G = 0.9$ to 1.0 kcal mol^{-1} for **4^{P}** complexes). In addition, variants containing substitution of a residue that contacts phosphoserine in the **KID^{P}**·KIX complex (Y658A, Y658F, and K662A) form complexes with **6^{U}** whose stabilities are significantly lower than the wild-type complex, despite the absence of a phosphoserine residue. Finally, the KIX variant whose **6^{U}** complex differs most significantly from that of the wild-type complex is I660A, in which the amino acid substituted is on the face of KIX opposite the **KID^{P}**-binding site, and does not contribute to the stability of the wild-type KID·KIX complex. The residues that contribute most heavily to recognition of **6^{U}** are widely scattered on the surface of KIX, suggesting that **6^{U}** may bind to KIX by wrapping around the protein, making contacts with both the α- and PPII-helix.

PPKID4^{P} Folding. The relative affinities of the eleven **4^{P}** variants for KIX indicate that a small core of residues located on the (presumably) interior face of the **4^{P}** α-helix (F20, L24 and Y27) contribute significantly to the affinity of this ligand for KIX. Substitution of each of these residues with alanine led to complexes with KIX that were 0.4 to 1.0 kcal mol^{-1} less stable than the wild-type complex. In addition, substitution of two residues located on the (presumably) interior face of the PPII helix (P5 and P8) with alanine led to complexes with KIX that were more than 0.3 kcal mol^{-1} less stable than the **4^{P}**·KIX complex. All of the side chains that contribute significantly or moderately to **4^{P}**·KIX complex stability, F20, L24, Y27, P5, and P8, lie at the center of the aPP hydrophobic core (Figure 4), consistent with a model in which the PPII helix in **4^{P}** folds on the α-helix upon binding to form an aPP-like structure. These results are not consistent with a model in which the PPII helix in **4^{P}** wraps around the KIX surface, making additional contacts similar to the KID helix A, as previously discussed;[1] in this case the side chains of residues F20, L24, and Y27 would be solvent-exposed and substitution with alanine should have little or no effect on KIX affinity. Additional support for a model in which the **4^{P}** hydrophobic core forms upon binding to KIX derives from differences in the effect of alanine and sarcosine substitutions along the PPII helix. Substitution of P5 or P8 with alanine eliminates the portion of the pyrolidine ring that would pack against α-helix residues F20 and Y27 (Figure 4). By contrast, substitution of P5 or P8 with sarcosine (P5Z and P8Z) retains the portion of the pyrolidine ring that would pack against α-helix residues F20 and Y27, allowing for hydrophobic packing. Both alanine and sarcosine are well-tolerated within a type II polyproline helix.[34,35] Therefore, the observation that the P5Z·KIX and P8Z·KIX complexes are more stable than the P5A·KIX and P8A·KIX complexes provides additional evidence that **4^{P}** folds into an aPP-like conformation upon binding to KIX, with residues P5, P8, F20, L24, and Y27 forming part of the hydrophobic core. It is possible that this folding energy represents the additional energetic factor contributing to the stability of the **4^{P}**·KIX complex but not the **KID^{P}**·KIX complex. We appreciate, however, that the differences in stability could also result from differences in conformation of the free ligands.

PPKID as Transcriptional Activators. Previously, Montminy and co-workers screened a phage library to identify an unphosphorylated peptide octamer (KBP 2.20) that bound KIX with a K_d of 16 μM and, when fused to a Gal4 DNA-binding domain, activated p300/CBP-dependent transcription approximately 40-fold. Analysis of a set of KBP variants suggested a direct correlation between the KIX binding affinity and transcriptional activation potential in this series.[22] A direct correlation between binding affinity and transcriptional potency has been suggested as a general model by a number of studies on activation domains. In one example, the equilibrium binding affinities of mutants of the yeast Gal4 activating region for transcriptional proteins TBP and TFIIB were shown to predict the extent of gene activation.[36] In a second example, the binding affinities and activation potential of a number of natural activation domains including Gal4, VP16, p53, GCN4, and Tat and non-natural activation domain AH were measured.[37] The results obtained suggested that the affinities of these activation domains for both transcriptional and nontranscriptional proteins were directly related to their transcriptional activation potencies. Our results are consistent with this model in the case of the phosphorylated KIX ligands **4^{P}** and **6^{P}**. Both **4^{P}** and **6^{P}** function as transactivation domains when fused to a Gal4 DNA-binding domain, eliciting levels of transcription in the presence of forskolin that are comparable to that elicited by the comparable KID construct under equivalent conditions. This equivalence in function is not surprising given the equivalence in binding mode, orientation, and overall affinity that we observe. In addition, **4^{P}** and **KID^{P}** give rise to similar transactivation profiles in the presence of additional p300, suggesting that transcription activation by both ligands occurs via the CBP/p300 pathway. More surprising is the observation that **6^{U}** fails to function as a transactivation domain when fused to a heterologous DNA-binding domain, despite its high affinity for KIX. The difference

(34) Rucker, A. L.; Creamer, T. P. *Protein Sci.* **2002**, *11*, 980.
(35) Nguyen, J. T.; Turck, C. W.; Cohen, F. E.; Zuckermann, R. N.; Lim, W. A. *Science* **1998**, *282*, 2088.
(36) Wu, Y.; Reece, R. J.; Ptashne, M. *EMBO. J.* **1996**, *15*, 3951.
(37) Melcher, K. *J. Mol. Biol.* **2000**, *301*, 1097.

in transcriptional activity between $\mathbf{6^U}$ and $\mathbf{6^P}$ may be attributed to the 2.5-fold difference in affinity for KIX.[1] However, the binding mode of $\mathbf{6^P}$ has not been investigated, and we cannot role out effects on transcriptional activity due to differences in binding mode. Interestingly, both $\mathbf{4^P}$ and $\mathbf{6^U}$ possess significantly higher affinity for KIX than KBP 2.20, yet they elicited a lower level of transcriptional activation. Analysis of the binding footprint of KBP 2.20 on KIX revealed that the peptide bound an overlapping yet minimal surface of KIX as compared to phosphorylated CREB or unphosphorylated KIX ligand c-Myb. Moreover, KBP 2.20 appeared to penetrate further into the hydrophobic groove. Taken together with the data for $\mathbf{6^U}$ and $\mathbf{6^P}$, the results suggest that although KIX affinity plays a role in determining the level of transcriptional activation mediated by a particular ligand, it is not the sole criterion. In fact, many factors may affect transcriptional activation potential including the lifetime of the ligand·CBP complex, the orientation of ligand binding, the resulting accessibility of CBP for binding to other essential transcription proteins, the rate of modification (phosphorylation), and susceptibility of the activator to degradation pathways in the cell. It is possible that $\mathbf{4^P}$, $\mathbf{6^U}$, and related molecules could be used to differentiate among these factors and provide key details for a general mechanism of transcription activation.

Conclusions

Equilibrium binding experiments using a panel of well-characterized KIX variants support a model in which $PPKID4^P$ ($\mathbf{4^P}$) binds KIX in a manner that closely resembles that of $KID\text{-}AB^P$ ($\mathbf{KID^P}$) but $PPKID6^U$ ($\mathbf{6^U}$) binds an overlapping yet distinct region of the protein. Equilibrium binding experiments using a judiciously chosen panel of $\mathbf{4^P}$ variants containing alanine or sarcosine substitutions along the putative α- or PPII helix of $\mathbf{4^P}$ support a model in which $\mathbf{4^P}$ folds into a pancreatic fold structure upon binding to KIX. Transcriptional activation assays performed in HEK293 cells using GAL4 DNA-binding domain fusion proteins of PPKID4 and PPKID6 indicate that $\mathbf{4^P}$ functions as a potent activator of p300/CBP-dependent transcription. $\mathbf{6^U}$ is a less potent transcriptional activator in this context than $\mathbf{4^P}$ despite the similarity of their affinities for KIX. This final result suggests that thermodynamic binding affinity is an important, although not exclusive, criterion controlling the level of CBP-dependent transcriptional activation.

Acknowledgment. This work was supported by the NIH (GM 65453) and in part by a grant to Yale University, in support of A.S., from the Howard Hughes Medical Institute. We are grateful to Jennifer Nyborg and Marc Montminy for generously providing the wild-type KIX and KIX variant expression vectors and John Frangioni for providing the pAL_1 plasmid and G5B Luciferase reporter plasmid. Oligonucleotide synthesis, DNA sequencing, and amino acid analysis were performed by the W. M. Keck Foundation Biotechnology Resource Laboratory at Yale University School of Medicine, New Haven, CT.

Supporting Information Available: All experimental protocols and western blot analysis of Gal4-PPKID fusion protein expression in HEK293 cells. This material is available free of charge via the Internet at http://pubs.acs.org.

JA042761Y